Available online at www.sciencedirect.com
SCIENCE DIRECT
ELSEVIER
Polymer 46 (2005) 7436–7442
polymer
www.elsevier.com/locate/polymer

Role of adsorbed iodine into poly(vinyl alcohol) films drawn in KI/I_2 solution

Tsukasa Miyazaki[a,*], Shigeru Katayama[a], Eiji Funai[b], Yoshihiro Tsuji[b], Shinich Sakurai[b]

[a]*Core Technology Center, Nitto Denko Corporation, 1-1-2, Shimohozumi, Ibaraki, Osaka 567-8680, Japan*
[b]*Department of Polymer Science and Engineering, Kyoto Institute of Technology, Matsugasaki, Sakyo-ku, Kyoto 606-8585, Japan*

Received 19 November 2004; received in revised form 6 May 2005; accepted 15 May 2005
Available online 28 June 2005

Abstract

We have investigated the microstructure of the poly(vinyl alcohol) (PVA) films using small- and wide-angle X-ray scattering (SAXS and WAXS, respectively) techniques. The samples were uniaxially drawn in water or KI/I_2 aqueous solution and then dried in an air-oven at 333 K for 1 h prior to SAXS and WAXS measurements. It was found that for the films drawn in KI/I_2 solution PVA chains in the microfibrillar structure are more extended upon the film drawing compared to the case of the films drawn in pure water, which is resulted from the correlation function analysis on the SAXS data. Adsorbed iodines into the film were anticipated to act as junction points between the microfibrils via the formation of the PVA-iodine complexes.

Keywords: Poly(vinyl alcohol); Small-angle X-ray scattering; Wide-angle X-ray scattering

1. Introduction

Poly(vinyl alcohol) (PVA) has been widely used in various industrial applications, such as high quality polarizers, high strength fibers and so on [1]. In particular, PVA films are very suitable to the application to polarizers, because they have high ability of PVA-iodine complex formation in the film microstructure. When PVA films are soaked in KI/I_2 aqueous solution, adsorbed iodines are one-dimensionally aligned and surrounded with PVA chains with the film drawing, followed by the formation of PVA-iodine complexes, which show extremely high ability of dichromatic performance.

About ten years ago, Miyasaka et al. systematically investigated the microstructure of PVA in the presence of water or PVA-iodine complexes in the films [2]. They proposed a structural model of PVA films swollen with water, so-called 'Double network model' as schematically shown in Fig. 1. They supposed that the PVA film consists of microfibrils in which the crystalline lamellar and amorphous region alternating stacks, and the amorphous region between microfibrils (not shown in Fig. 1). Moreover, they assumed that the amorphous layer in the lamellar structure contains tie chains that interconnect crystallites. As there are two networks in their model, polymer chain network and fibrillar network, it is referred to as a double network model. They also proposed a structural model of a PVA-iodine complex, based on their experimental result that PVA-iodine complexes are preferentially formed in the amorphous region rather than the PVA crystalline phase, upon soaking PVA films in KI/I_2 aqueous solution at relatively low iodine concentrations [2,3]. In their model, the one-dimensional arrays of polyiodines are surrounded with some extent of extended PVA amorphous chains. Extension of PVA films remarkably enhances the PVA-iodine complex formation, implying that the model of the PVA-iodine complex proposed by Miyasaka et al. seems to be reasonable compared to other models previously proposed, such as the helix model [4,5]. A similar model was proposed by Takamiya et al. who suggested that polyiodines were surrounded with the aggregates of extended sequences in syndiotactic PVA chains [6].

Furthermore, Miyasaka et al. reported that Young modulus of PVA films become high upon soaking in KI/I_2 aqueous solution with a relatively low iodine concentration [2,7]. It can be therefore concluded that PVA-iodine complexes should act as junction points in the network of

* Corresponding author. Tel.: +81 72 621 0276; fax: +81 72 621 0307.
E-mail address: tsukasa_miyazaki@gg.nitto.co.jp (T. Miyazaki).

0032-3861/$ - see front matter © 2005 Elsevier Ltd. All rights reserved.
doi:10.1016/j.polymer.2005.05.129

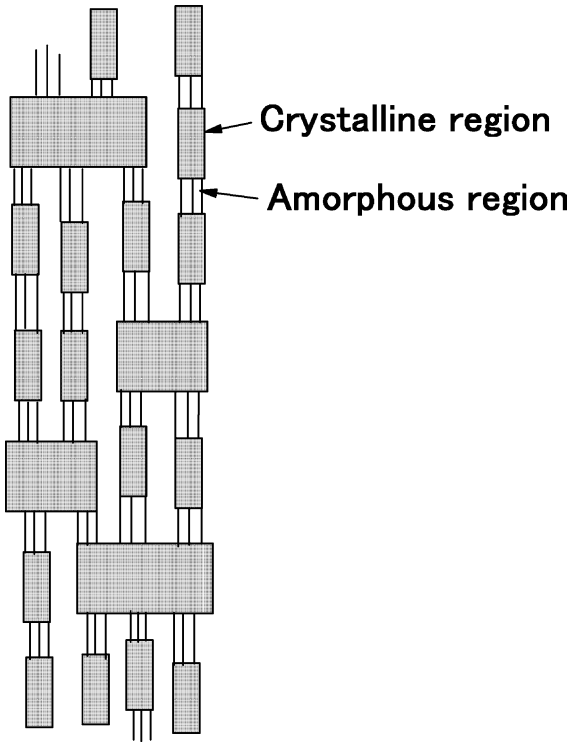

Fig. 1. Schematic diagram of a structural model for the PVA film swollen in water. The amorphous region between the microfibrils is not shown in the figure.

PVA chains in an amorphous phase [7]. It is expected that the increase of the junction points in the network leads to various microstructural changes and properties of polymers with the film drawing. In particular, many molecular chains may be effectively extended associated with the increase in the number of junction points in the fibrillar network in film drawing processes, because it is expected that the number of chains carrying the applied load increases with increasing the junction points.

Note here that the iodine concentration in the film can be widely controlled with the iodine concentration in solution. This fact implies that the control of the number of the junction points in the microfibrillar network can be conducted by externally changing the iodine concentration in solution. Since this procedure hardly alter the microstructure of PVA films, this promisingly leads to the development of polymers with various extents of mechanical toughness. Therefore, in this article, we focus on and clarify the roles of the iodines adsorbed into PVA films as junction points in the microfibrillar network, such that PVA-iodine complexes contribute to the effective extension of the PVA chains in the film drawing process.

2. Experimental

The PVA films made by Kuraray Co. (Vinylon) with the degree of polymerization of 2400 were used in this study. The triad tacticity (mm = 0.21, mr = 0.51, rr = 0.28) was determined by solution state 1H NMR spectroscopy. The films also had a high degree of saponification, >98 mol%. The films were subjected to uniaxial drawing in pure water or in aqueous solution of 0.05 wt% KI/I_2 (KI:I2 = 5:1) up to a desired draw ratio in 3 min, followed by drying in an air-oven at 333 K for 1 h. The thickness of the undrawn film was 0.075 mm, and the thickness of the drawn films was 0.02–0.05 mm depending on the draw ratio. Only a small amount of iodine (<3 wt%) was adsorbed in the films drawn in KI/I_2 aqueous solution, which was determined by X-ray fluorescence spectroscopy. Light brown colored PVA film was obtained when the film was soaked in KI/I_2 aqueous solution without drawing the film, indicating that iodine was adsorbed in the film, but no complex was formed because the iodine concentrations were too law. When the films were drawn in KI/I_2 solution, they changed the color from light brown to light blue during extension, showing that a small amount of the complex was formed in the films [2]. The uniformity in coloring of the film in the film thickness direction was confirmed with optical microscopy.

The structure of the dried films was analyzed by small- and wide-angle X-ray scattering (SAXS and WAXS, respectively) techniques. SAXS experiments were performed with the SAXS apparatus on BL40B2 beamline at Spring-8. The wavelength used was 0.1 nm or 0.15 nm. The camera length of the SAXS apparatus was about 1000 mm. WAXS experiments were conducted using laboratory equipments with a pinhole camera on the rotating anode X-ray generator. The wavelength used was 0.154 nm. The camera length of the WAXS camera was 70 mm. On both experiments, imaging plate X-ray detector systems were used for the measurements of two-dimensional (2-D) scattering patterns from the samples. The exposure time was 30 min for WAXS measurements. For SAXS measurements, the exposure time was 5–10 min even on the synchrotron SAXS camera for the detailed analysis mentioned below.

3. Results and discussion

Fig. 2(a) and (b) shows the typical examples of the 2-D SAXS patterns of the films drawn in pure water and KI/I_2 aqueous solution, respectively. Here, q denotes the magnitude of the scattering vector and defined by $q = (4\pi/\lambda)\sin\theta$ with λ and 2θ being the wavelength of X-ray and scattering angle, respectively. Fig. 3 shows corresponding 2-D WAXS patterns of the same films. Here, we could not identify the scattering from the structure of polyiodine or PVA-iodine complex in the 2-D SAXS patterns for the films drown in KI/I_2 solution. It may be ascribed to a small amount of the iodine in the films. As a matter of fact, 2-D SAXS patterns for the films drawn in KI/I_2 solution are essentially the same as those for the films drawn in pure water.

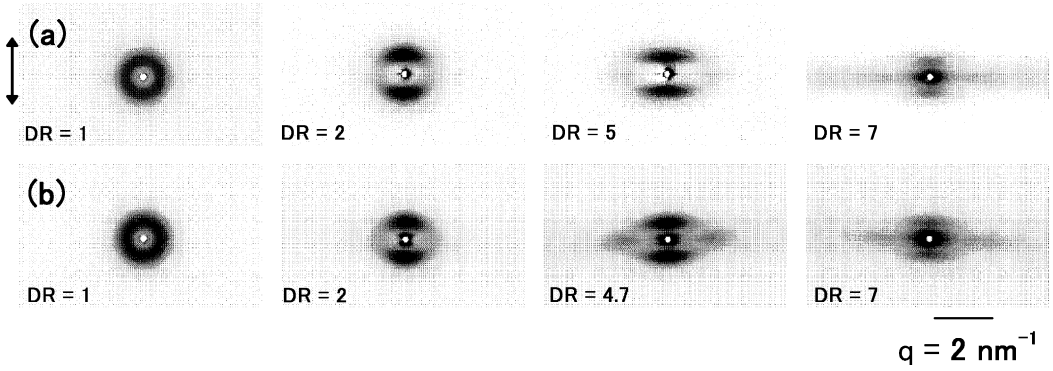

Fig. 2. Two dimensional small angle X-ray scattering patterns for the films drawn in pure water (a) and in KI/I_2 solution (b) with the draw ratio (DR) indicated in the figures. The arrow indicates the draw direction.

The stack of crystalline lamellar phase is preferentially repeating in the draw direction upon drawing and the tendency is more exaggerated with increasing the draw ratio as shown in the 2-D SAXS patterns. Two crystalline peaks ((101), (10$\bar{1}$) doublet and (200), the latter peak appears to be a shoulder peak of the former) appear to the equatorial direction in the 2-D WAXS patterns. This is consistent with the lamellar orientation observed in the SAXS patterns with the film drawing.

The correlation function analysis [8] is adopted to quantitatively analyze the lamellar structure oriented to the draw direction. The correlation function $\gamma(r)$ is calculated from the scattering intensity as

$$\gamma(r) = \frac{\int_0^\infty I_{cor}(q)\cos(qr)\mathrm{d}q}{Q}$$

where $I_{cor}(q)$ is the Lorentz-corrected intensity, which is given by multiplying the observed meridional intensity by q^2 and Q is the invariant defined as

$$Q = \int_0^\infty I_{cor}(q)\mathrm{d}q$$

A typical shape of the correlation function is shown in Fig. 4 for the film drawn in pure water with the draw ratio of 5.7. The position of the first maximum (d_{max}) corresponds to the long period (lamellar periodicity), while the position of the first minimum (d_{min}) very closely corresponds to the lamellar crystalline thickness or the intermediated amorphous region thickness. Fig. 5 shows d_{max}, d_{min} and their difference (d_{max}–d_{min}) with the draw ratio for the films drawn in pure water and KI/I_2 aqueous solution.

We estimated the crystallinity index of the drawn films from the 2-D WAXS patterns in order to determine whether the d_{min} value corresponds to the crystalline or amorphous thickness from the correlation function. The azimuthally integrated intensity profile of 2-D WAXS patterns versus

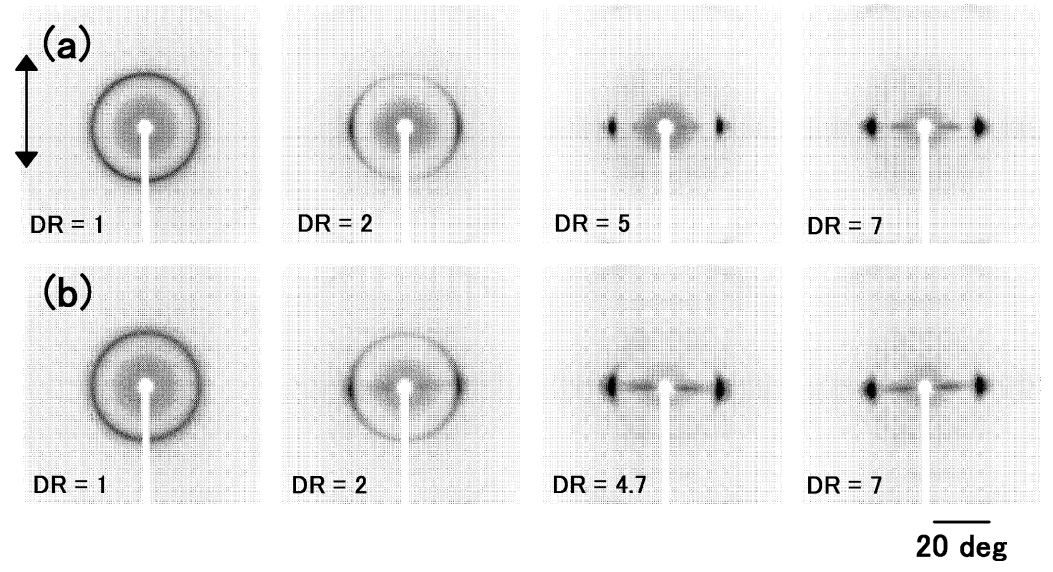

Fig. 3. Two dimensional wide angle X-ray scattering patterns for the films drawn in pure water (a) and in KI/I_2 solution (b) with the draw ratio (DR) indicated in the figures. The arrow indicates the draw direction.

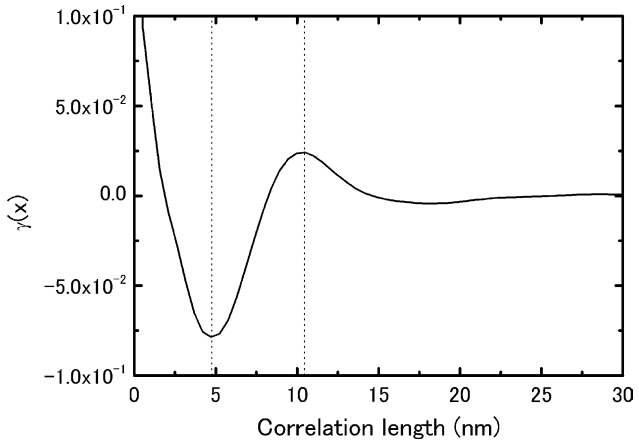

Fig. 4. Typical example of the one dimensional correlation function for the meridional slice of a 2-D SAXS pattern for the film drown in pure water with a draw ratio of 5.7.

the scattering angle is used for this analysis. Fig. 6(a) shows the azimuthally integrated intensity profiles for the films undrawn in pure water and in KI/I_2 aqueous solution. These profiles seem to be perfectly identical, attributed to a small amount of iodine in the films undrawn in KI/I_2 solution. However, for the drawn films with a high draw ratio (Fig. 6(b)), for the films drawn in KI/I_2 solution the profiles are different from those of the films drawn in water in the range of about $2\theta = 27$–$35°$, which is due to the scattering

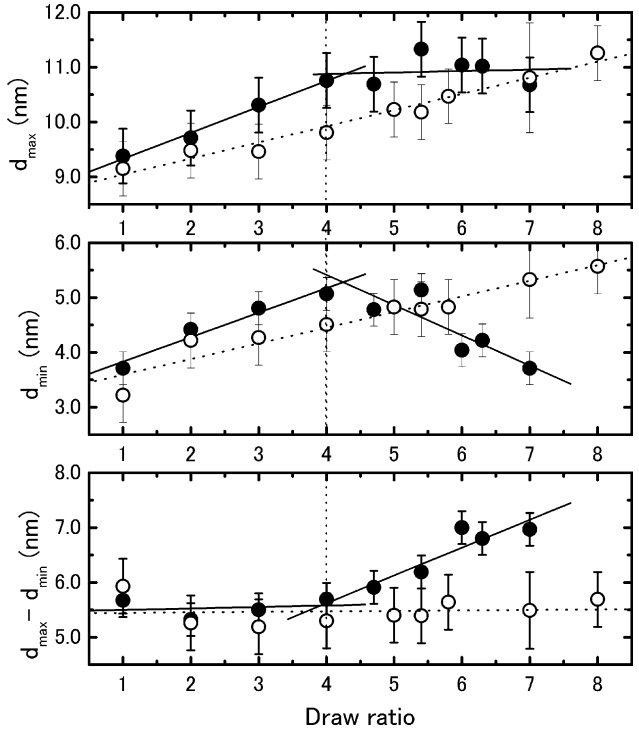

Fig. 5. Draw ratio dependence of d_{max} (long period), d_{min} (identified to the amorphous region thickness) and d_{max}–d_{min} (identified to the crystalline thickness) for the films drawn in pure water (○) and in KI/I_2 solution (●) derived from the one dimensional correlation function typically shown in Fig. 4.

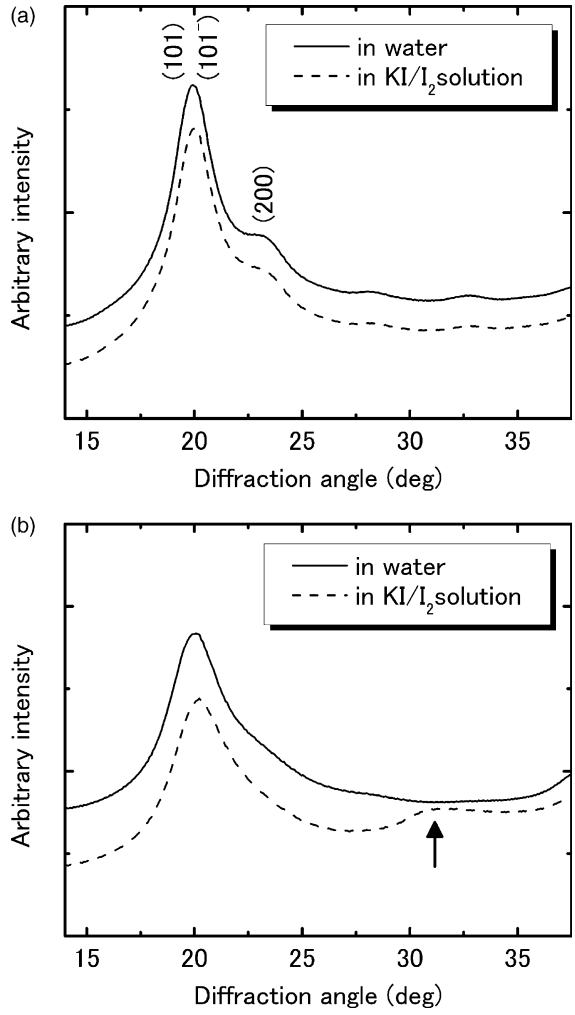

Fig. 6. (a) Azimuthally integrated intensity profiles of 2-D WAXS patterns for the films undrawn in water (solid line) and in KI/I_2 aqueous solution (dashed line), (b) for the films drawn in water (solid line) and in KI/I_2 aqueous solution (dashed line) with the draw ratio of 7.

peak localized at about $2\theta = 30°$, as indicated by an arrow in this figure. The scattering peak localized in this range is thought to be originated from the mean bond length between the iodine atoms in polyiodine complexes aligned parallel to the draw direction, as shown in the layer lines in the meridian direction in Fig. 3(b). However, for the range below $2\theta = 27°$, differences in the scattering profiles can be negligible. Therefore, we estimate the crystallinity of the samples with the peak decomposition method on the scattering profiles in the range of $2\theta = 15$–$27°$ for convenience.

In peak fitting procedure, only one fixed parameter is the full width at half maximum (FWHM) of the amorphous peak, which can be evaluated from the meridian slice of the 2-D WAXS pattern for the fully drawn film because no crystalline reflection appears in the meridian. Other parameters (positions, heights and FWHMs of the two crystalline peaks and position and height of the amorphous peak) are floated in the fitting routine. The crystallinity

index, f_c is thus determined as follows:

$$f_c = \frac{\sum A_c}{\sum A_c + A_a}$$

where A_c is the integrated area underneath the crystalline peaks and A_a is the integrated area of the amorphous peak. A typical example of the peak decomposition is shown in Fig. 7. The peak positions of (101), (10$\bar{1}$) reflection and (200) reflection are $2\theta = 19.9$ and $2\theta = 23.6°$, respectively, agreed with the previous reported values [9]. Fig. 8 shows the crystallinity index, f_c of the films drawn in pure water and KI/I_2 aqueous solution with the draw ratio. This f_c can only be used to compare samples within this experiment only for qualitative trends, and it should be considered that the value of f_c differs from the absolute crystallinity of the PVA samples. For example, the accurate crystallinity of PVA films can be estimated with the method proposed by Sakurada et al. [10–12]. Their method could not be applicable to our limited data, as described above. However, for the film undrawn in pure water, the crystallinity index, 34% determined using our convenient X-ray method described above is well consistent with the value, 32% determined by the density obtained with the floating method. Note here that other determination methods of the crystallinity such as the density measurement method are not applicable, because a small amount of iodine adsorbed in the sample drawn in KI/I_2 solution may overestimate the measured density value depending on the draw ratio.

As shown in Fig. 5, for the films drawn in pure water, the long period d_{max} is expanded linearly with the draw ratio. Interestingly, it is found that the d_{max}–d_{min} is almost constant irrespective of the draw ratio. This means that the increase in the long period d_{max} is attributed to the expansion of d_{min}. In the case of the films drawn in pure water, the f_c value decreases with increasing the draw ratio, seems to allow us to assign d_{min} and d_{max}–d_{min} derived from

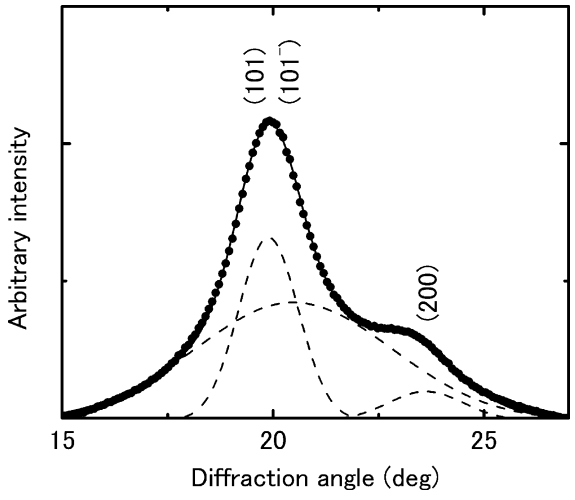

Fig. 7. Typical example of the peak decomposition of an azimuthally integrated intensity profile for a 2-D WAXS pattern. Points are experimental data. Lines are the best fitting curves.

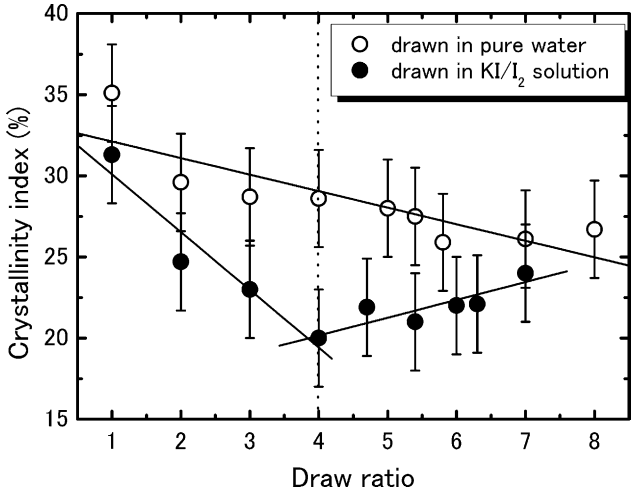

Fig. 8. Draw ratio dependence of the crystallinity index, f_c for the films drawn in pure water (○) and in KI/I_2 solution (●).

the one dimensional auto correlation function analysis of the SAXS profile to the amorphous region thickness and the crystalline phase thickness, respectively. It is well known that the lamellar thickness can be undoubtedly determined by the size of the crystalline in the molecular chain direction, which can be possibly estimated by applying Scherrer equation to (020) reflection in the case of PVA films. However, relatively high angle diffraction peaks such as (020) reflection are not clearly detected for our samples, especially with a law draw ratio, which is due to a law crystallinity.

The assignment of d_{min} to the amorphous region thickness is consistent with the fact that the amorphous region is easily expanded but the crystalline phase is hard to be expanded by the film drawing. As mentioned below, the decrease in the crystallinity, f_c should be attributed to the structural change from the lamellar structure to the microfibrillar structure associated with the lamellar breakup with the film drawing. The small crystallinity index (20–30%) compared to the apparent crystallinity index in the lamellar stack ($(d_{max}–d_{min})/d_{max}$) must be attributed to the large amount of amorphous region between the lamellar stacks or the microfibrils.

For the films drawn in KI/I_2 aqueous solution, below the draw ratio of about 4, the expansion of the lamellar structure is much larger than that of the films drawn in pure water and is also attributed to expansion of d_{min}, as observed in the case of the films drawn in pure water. This indicates that d_{min} may be also assigned to the amorphous region thickness and the microfibrils in the films are effectively expanded below the draw ratio of 4, as compared to those in the films drawn in pure water. However, above the draw ratio of about 4, the long period is not affected on the film drawing by the compensation of the increase in d_{max}–d_{min} and the decrease in d_{min}, as shown in Fig. 5.

In the case of the films drawn in KI/I_2 aqueous solution, below the draw ratio of about 4, the f_c value substantially

decreases with increasing the draw ratio, followed by the gradual increase in f_c with the film drawing above the draw ratio of about 4 as shown in Fig. 8. This behavior is consistent with the correlation function analysis results of the lamellar structure, because firstly d_{min} (identified to the amorphous region thickness as mentioned above) increases with increasing the draw ratio below the draw ratio of about 4, and then the decrease in d_{min} and the increase in $d_{max}-d_{min}$ (identified to the lamellar crystalline thickness) are observed with the film drawing above the draw ratio of about 4. The increase in the crystalline thickness should be attributed to the 'strain induced crystallization' by the large orientation of the tie molecules in the amorphous region with the film drawing [13]. Strain induced crystallization only occurs in the films drawn in KI/I_2 solution, indicating that the tie molecules in the amorphous region can be effectively stretched and that the microfibrils in the films drawn in KI/I_2 aqueous solution effectively bear the applied stress compared to those in the films drawn in pure water at the same draw ratio. The iodines adsorbed into the film form the PVA-iodine complexes and are considered to play a role of structuring the microfibrillar network through working as junction points between the microfibrils.

The equatorial streak scattering is observed in the 2-D SAXS patterns for the films with a high draw ratio. Moreover, there is a peak in the streak scattering, as typically observed in Fig. 2 (b) for the film drawn in KI/I_2 solution at the draw ratio of 4.7. The equatorial streak seen in the 2-D SAXS pattern can arise from a variety of sources [14]. This scattering may be originated from the inter-particle interference of the microfibrils, because the scattering intensity is comparable to the meridional peaks originated from the repeating lamellar structure whereas it is very weak as compared to the equatorial and meridional streak scattering observed at much lower scattering angle for the films with a high draw ratio, which may be due to voids or cracks with the film drawing [14]. The correlation length related to the equatorial streak scattering is evaluated from the Lorentz-corrected intensity profile for the equatorial slice using the Bragg's low. Fig. 9 shows the draw ratio dependence of the correlation length. The value is below about 6 nm and decreases with increasing the draw ratio. It is noted here that the decrease in the correlation length is more exaggerated for the films drawn in KI/I_2 aqueous solution as compared to those drawn in pure water.

The microfibril diameter can be estimated from the crystallite size in the direction perpendicular to the draw direction. For this estimation, the equatorial slice of the 2-D WAXS pattern is plotted and decomposed into two crystalline peaks and one amorphous peak, such as carried out for the determination of the f_c. The FWHM of the (101) and (10$\bar{1}$) doublet is used to obtain the averaged crystallite size, l_c corresponded to the microfibril diameter using the Scherrer equation

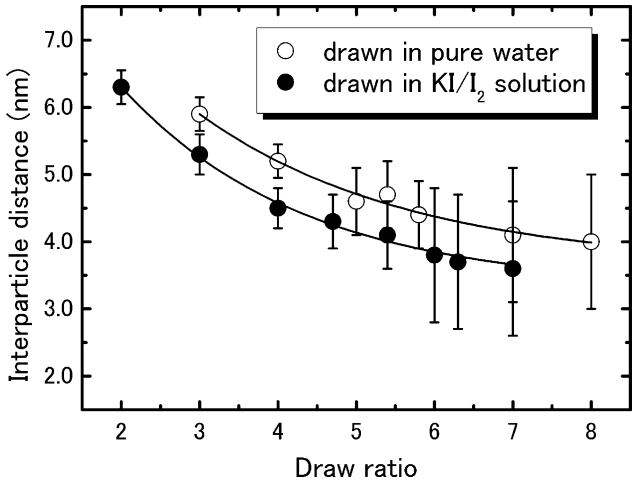

Fig. 9. Draw ratio dependence of the interparticle distance of the microfibrils derived from the peak position of the equatorial streak scattering using the Bragg's law for the films drawn in pure water (○) and in KI/I_2 solution (●).

$$l_c = \frac{0.9\lambda}{(\Delta 2\theta)\cos\theta_m}$$

where $\Delta 2\theta$ is the FWHM of the crystalline peak in radian, θ_m is the peak angle. Fig. 10 shows the draw ratio dependence of the l_c for the films drawn in pure water and KI/I_2 aqueous solution. As shown in Fig. 10, the microfibril diameter estimated from the crystallite size in the direction perpendicular to the draw direction is comparable to or larger than the correlation length expected as the inter-particle distance of the microfibrils, indicating that the microfibrils must be densely packed and there must be many crystallites, which size is larger than the microfibril diameter, as the junction points in the fibrillar network as shown in Fig. 1. The large reduction in the crystallite size between the draw ratio of 1 and 2 must be attributed to the

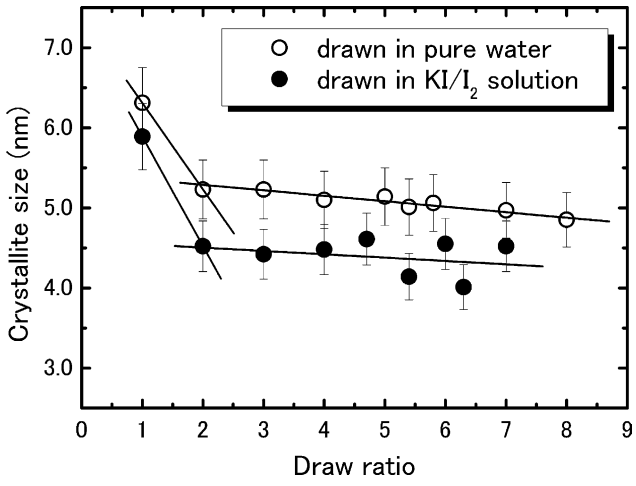

Fig. 10. Draw ratio dependence of the crystallite size, l_c for the films drawn in pure water (○) and in KI/I_2 solution (●) using the diffraction of the (101), (10$\bar{1}$) doublet oriented to the direction perpendicular to the draw direction.

structural change from the lamellar structure to the microfibrillar structure associated with the lamellar breakup. Much larger decrease in the crystallinity index and the interparticle distance of the microfibrils is observed before the occurrence of the strain induced crystallization for the films drawn in KI/I_2 aqueous solution compared to the films drawn in pure water, also indicating that adsorbed iodines producing the PVA-iodine complexes act as junction points between the microfibrils in the film and contribute to the effective extension of the PVA chains in the microfibrils. These PVA-iodine complexes have not only a high dichromatic performance but also an important role in PVA for the development of a high strength fiber.

4. Conclusion

In this study, we demonstrated that adsorbed iodines into the amorphous region of the PVA film act as junction points between the microfibrils via the formation of the PVA-iodine complexes and contribute to the structuring of the microfibrillar network. In the results, the PVA chains in the film are effectively extended with increasing the draw ratio.

Acknowledgements

The authors wish to thank Prof K. Sakurai, Dr I. Akiba of The University of Kitakyushu and Dr K. Yamamoto of Nagoya Institute of Technology for their support on our experiments at Spring-8. The synchrotron radiation experiments were performed at the Spring-8 with the approval of the Japan Synchrotron Radiation Research Institute (JASRI) (Proposal No.2004A0104-CL2b-np).

References

[1] Sakurada I. Polyvinyl alcohol fibers. New York: Marcel Dekker; 1985.
[2] Miyasaka K. Adv Polym Sci 1993;108:91.
[3] Choi YS, Miyasaka K. J Appl Polym Sci 1993;48:313.
[4] Zwick MM. J Appl Polym Sci 1965;9:2393.
[5] Inagaki F, Harada I, Shimanouchi T, Tasumi M. Bull Chem Soc Jpn 1972;45:3384.
[6] Takamiya H, Tanahashi Y, Matsuyama T, Tanigami T, Yamaura K, Matsuzawa S. J Appl Polym Sci 1993;50:1807.
[7] Kojima Y, Furuhata K, Miyasaka K. J Appl Polym Sci 1985;30:1617.
[8] Strobl GR, Schneider M. J Polym Sci, Polym Phys 1980;18:1343.
[9] Choi YS, Oishi Y, Miyasaka K. Polym J 1990;22:601.
[10] Sakurada I, Nukushina Y, Mori N. Kobunshi Kagaku 1955;12:302.
[11] Sakurada I, Nukushina Y, Mori N. Kobunshi Kagaku 1955;12:307.
[12] Sakurada I, Nukushina Y, Mori N. Kobunshi Kagaku 1955;12:311.
[13] Samon JM, Schultz JM, Hsiao BS. Polymer 2000;41:2169.
[14] Wu J, Schultz JM, Yeh F, Hsiao BS, Chu B. Macromolecules 2000; 33:1765.